

---

# Pruning Large Language Models with Semi-Structural Adaptive Sparse Training

---

**Weiyu Huang**  
Tsinghua University

**Guohao Jian**  
Tsinghua University

**Yuezhou Hu**  
Tsinghua University

**Jun Zhu**  
Tsinghua University

**Jianfei Chen**  
Tsinghua University

## Abstract

Transformer-based Large Language Models (LLMs) have demonstrated remarkable success across various challenging tasks. However, the deployment of LLMs is hindered by their substantial parameter count and memory consumption. Recently, numerous studies have attempted to compress LLMs by pruning them using training-free methods. However, these pruned models often experience significant performance degradation on complex tasks. To address this issue, we propose a novel training pipeline for semi-structured sparse models, named Adaptive Sparse Trainer (AST). By distilling the knowledge stored in its dense counterpart, we prevent the sparse model from overfitting and ensure a stable training process. Moreover, AST allows the model to adaptively select better lottery tickets (e.g., masks) during training. Additionally, we discovered that adding extra well-initialized parameters can further enhance model performance with only a small increase in memory footprint. Our method significantly narrows the performance gap between dense and sparse models while maintaining limited computational cost. Furthermore, when combined with existing quantization methods, AST can compress language models by up to 16x compared to dense FP32 precision models with minimal performance loss. AST outperforms previous state-of-the-art methods by reducing the zero-shot accuracy gap between dense and semi-structured sparse models to 1.12% across multiple zero-shot tasks on Llama2-7B, using less than 0.4% of the pretraining tokens.

## 1 Introduction

Transformer-based Large Language Models (LLMs) [1, 4, 7] have achieved tremendous success across various challenging tasks. However, the inference speed of current state-of-the-art models is limited due to their enormous parameter count and memory latency. Therefore, it is crucial to find viable model compression methods to reduce memory footprint and lower the deployment barrier.

Model pruning [9, 14, 45] is an effective method to compress LLMs by setting a proportion of weights to zero to satisfy a certain sparsity pattern. Recently, N:M sparsity has emerged as a type of semi-structured sparsity, offering a good balance between precision and efficient hardware support. Specifically, N:M sparsity retains only N nonzero elements out of each group of M elements. This sparsity pattern can accelerate both matrix multiplication and memory access, potentially enhancing the performance of both prefilling and decoding processes on off-the-shelf GPUs.

Existing state-of-the-art N:M pruning methods for LLMs, such as SparseGPT [9] and Wanda [45], adopt a post-training approach to compute the connectivity pattern and update retained weights in a layer-by-layer fashion, without the need for back propagation. Despite their efficiency, these methods

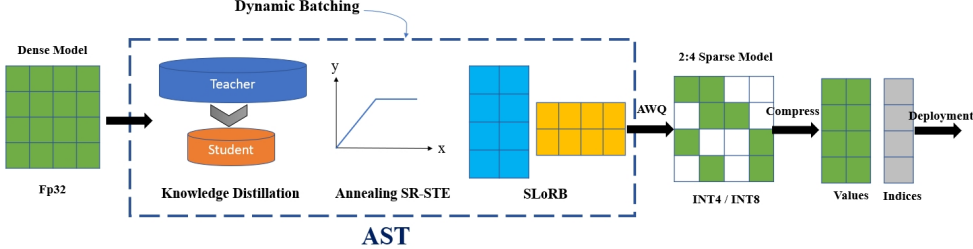


Figure 1: Workflow of deploying models with 2:4 sparsity pattern: (a) We use AST to train semi-structured sparse model from its dense counterpart. (b) We use AWQ to quantize model into lower precision. (c) We store compressed model weight by keeping tract of non-zero element and indices.

still encounter considerable performance degradation. Moreover, recent findings show that in more challenging tasks requiring complex knowledge and comprehension, current pruning methods fail completely even at relatively low sparsity [23], raising concerns about the feasibility of pruning LLMs.

In this work, we show that semi-structured sparse LLMs can achieve competitive performance not only on perplexity but also on complex zero-shot and few-shot tasks for the first time. Specifically, we directly retrain dense pretrained LLMs into sparse ones. While there has been considerable work on retraining pruned models, most focus on downstream tasks or smaller models with limited generalization capabilities [15, 44]. To our knowledge, we are the first to apply retraining on LLMs with billions of parameters and evaluate their performance on zero-shot tasks. We named our setting as *Post-Prune Retraining for Generalization (PRG)*. However, conducting PRG on LLMs presents significant challenges: 1) due to the unavailability of the original pretraining dataset, only weaker open-source datasets can be used for retraining, which could lead to catastrophic forgetting and the loss of emergent abilities; and 2) compared to one-shot pruning methods, retraining incurs heavy computational costs.

To address the challenges mentioned above, we propose **Adaptive Sparse Trainer (AST)** for training semi-structured sparse LLMs. First, instead of permanently setting all pruned weights to zero at the start of training, AST gradually decays unimportant weights to zero while allowing pruned weights to revive during training. This approach enables the model to transition smoothly from a dense to a sparse state, benefiting the training process while finding the most suitable global connectivity pattern. This approach enables the model to transition smoothly from a dense to a sparse state, benefiting the training process while finding the most suitable global connectivity pattern. This approach also ensures that the sparse model retains the valuable world knowledge and performance characteristics of the original dense model, enhancing its generalization ability. Furthermore, we add a relatively small proportion of carefully initialized parameters to further enhance model performance. Finally, to minimize the gap caused by the pretraining dataset, we use the open-sourced Red-Pajamas dataset combined with dynamic batching [48]. We find that AST can fully unleash the potential of sparse models. When used to train a 2:4 sparse model from dense LLAMA2-7B, we achieved minimal performance loss: an increase of 0.6 in perplexity and a 1.2% accuracy drop in zero-shot results with minimal training tokens (less than 0.4% of pretraining tokens). We further compress our model using AWQ quantization method and obtained competitive models with state-of-the-art compression rate. Our complete workflow for compressing models is shown in Figure 1.

## 2 Related Work

**Network Pruning** Pruning is a crucial technique aimed at reducing model size and computational requirements while maintaining performance. It originated from methods like Optimal Brain Damage [29] and Optimal Brain Surgeon [17]. Based on sparsity patterns, pruning methods can be broadly categorized into unstructured, structured, and semi-structured pruning. Unstructured pruning removes individual weights [14, 38], which can maintain performance even with high sparsity. However due to its random pattern, unstructured models are difficult to accelerate. Structured pruning [31, 35, 36, 43], on the other hand, removes entire neurons, filters, or attention heads, resulting in models that are easier to accelerate on standard hardware but often suffer from severe performance loss. Recently,

semi-structured sparsity (e.g., N:M sparsity) [22] has been applied as a trade-off between performance and achieving actual speedup. While earlier works mostly focused on small discriminative models such as ResNets, recently a series of works [9, 45, 51, 52] have made progress in pruning LLMs with billions of parameters. However, these methods still fall short in zero-shot performance with semi-structured sparsity.

**Retraining Pruned Models** Another line of approach [32, 41, 54] focuses on retraining pruned models for better performance. While retraining techniques work well on smaller models with simpler tasks [27, 55], their application to large-scale models is limited because the training process demands substantial computational resources. Recently, Sheared LLaMA [48] employed a two-stage structured pruning process to train models that outperform other models of similar size. Our work, however, focuses on the retraining of semi-structured sparse large language models.

**Model Compression Methods** Compressing models can save memory footprint and speed up inference during deployment. Earlier methods like Deep Compression [14] combine pruning, quantization, and Huffman coding to significantly reduce the size of neural networks. More recent work like [9, 13, 45] has combined sparsity with quantization on large language models. In our work, we combined state-of-the-art quantization methods [30] with our semi-structured sparse model.

### 3 Preliminary

In this section, we present the mathematical formulation for model pruning and review some related work on training sparse models.

#### 3.1 Sparsity in Transformer-Based Model

To preserve model performance while inducing sparsity, the common practice in pruning transformer-based models is to prune all the linear layers in both attention and MLP blocks. As a formulation, we consider the matrix multiplication for linear layer:

$$Z = XW^\top, Z \in \mathbb{R}^{N \times D}, X \in \mathbb{R}^{N \times C}, W \in \mathbb{R}^{D \times C}.$$

Where  $X, W, Z$  are model input, weight matrix, and output activation respectively. Pruning model is equivalent to multiplying element-wise masks to model weight:

$$\tilde{W} = m(W) \odot W, m(W) \in \{0, 1\}^{D \times C}$$

Previous work has extensively studied the criteria for selecting the mask  $m(W)$  [8, 9, 16, 45]. In the context of our paper, where the mask is being recalculated during forward pass we find that the *classic magnitude criteria still outperforms other one-shot pruning methods*. This aligns with previous findings [37] and is attributed to two main reasons: First, most one-shot pruning methods have quadratic or cubic complexity with respect to the hidden dimension size, introducing significant computational overhead during training. Secondly, we observe that incorporating activation levels into the pruning metric is counterproductive during training, as activation levels may fluctuate due to weight updates. This variability renders the criteria less accurate in the later stages of training.

In this work, we focus on N:M sparsity [22], where the sparsity is restricted to having  $N$  nonzero elements in every  $M$  consecutive weights that are connected to the same output.

#### 3.2 Training Sparse Model

When implementing the backward pass for a sparse model with automatic differentiation, the gradient cannot flow through the mask  $m(W)$  due to its discrete nature. A common approach to circumvent this problem is to use straight through estimator (STE) [2] or its variant Sparse-Refined STE (SR-STE) [53]. STE allows the gradient to pass to the weights  $W_t$  by ignoring masking operation in the backward pass and updates parameters with gradient with respect to masked weight  $\tilde{W}_t$ , where  $W_t$  is the parameter in the  $t$ -th iteration:

$$W_{t+1} \leftarrow W_t - \gamma_t g(\tilde{W}_t)$$

In practice, the gradients from STE are often inaccurate due to approximation. Therefore latter work uses SR-STE as a refined version of STE, which penalizes weights with zero mask,

$$W_{t+1} \leftarrow W_t - \gamma_t (g(\tilde{W}_t) + \lambda_W \overline{m(W_t)} \odot W_t)$$

Recent work [21] proposes adding decay to the gradient when using the Adam optimizer [25] to avoid the oscillation of masks,

$$g_t \leftarrow \tilde{g}_t + \lambda_W \overline{m(W_t)} \odot W_t$$

$$W_{t+1} \leftarrow W_t - \frac{\gamma(u_t \beta_1 + (1 - \beta_1)g_t)}{(1 - \beta_1^t)(\sqrt{v_t} + \epsilon)}$$

Where  $\tilde{g}_t$  is gradient of  $\tilde{W}_t$ ,  $u_t$  and  $v_t$  are the first-order and second-order momenta, respectively.

### 3.3 Measuring Training Stability

Several metrics are introduced to measure the stability of masks during training, such as flip rate [21] and SAD [53]. In this paper, we primarily measure the flip ratio and the initial flip ratio, which respectively quantify the mask changes between the current step and the previous step, as well as between the current step and the initial step.

$$r_t = \|m(W_t) - m(W_{t-1})\|_1 / D$$

$$i_t = \|m(W_t) - m(W_0)\|_1 / D$$

Where  $D$  represents the total parameter count in the linear layer. A higher flip rate indicates that the mask is changing more rapidly, while a lower flip ratio suggests that the mask is more stable.

### 3.4 Knowledge Distillation

Knowledge distillation [12, 39] is a method used to train a smaller "student" model by learning from a larger "teacher" model to achieve comparable performance with reduced computational cost. This technique involves training the student to mimic the teacher's outputs using a specialized loss function. In our case, the student model is the sparse model and the teacher model is its dense counterpart. We experimented with different types of distillation losses.

*KL-divergence loss* [26] is used to measure the difference in the output probability distributions between the student and teacher models:

$$\mathcal{L}_{logit} = D_{KL}(\theta_t || \theta_s) = \frac{1}{B \times S} \sum_{i=1}^{B \times \text{seq}} p_{\theta_t}(x_i) \log \frac{p_{\theta_t}(x_i)}{p_{\theta_s}(x_i)}$$

Where  $B$  is the batch size,  $S$  is the sequence length,  $p_{\theta_t}$  and  $p_{\theta_s}$  are probability distributions of the teacher and student model, respectively.

*SquareHead Loss* [28] measures the difference of intermediate representation using mean squared error:

$$\mathcal{L}_{feat} = \frac{\text{MSE}(f_t^l, f_s^l)}{\text{MSE}(f_t^l, 0)}$$

Where  $f_t^l$  and  $f_s^l$  are the hidden state of  $l$ -th layer at step  $t$  for the teacher and student model, respectively.

## 4 Adaptive Sparse Trainer

In this section, we first identify the differences between classic pretraining and Post-Prune Retraining for Generalization (PRG), as well as the unique challenges associated with PRG. Based on our analysis, we then propose three methods to facilitate a robust PRG training process and obtain sparse models with state-of-the-art performance.

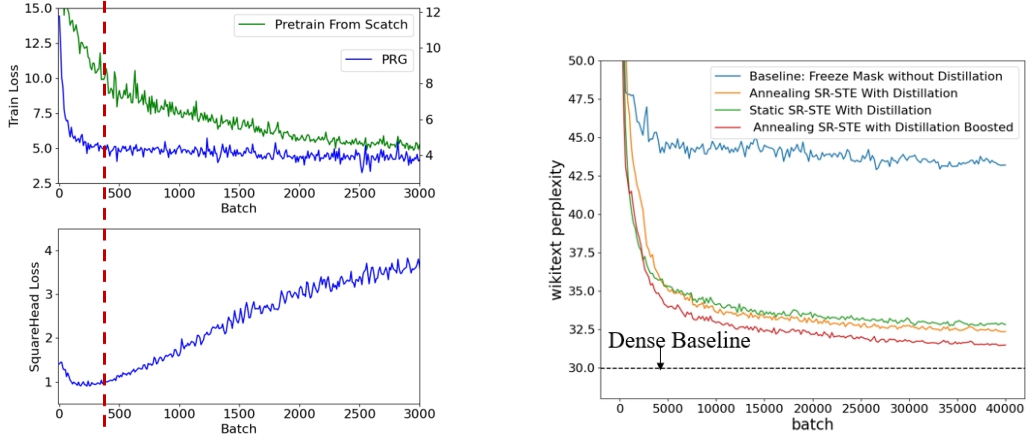


Figure 2: **(Left)** Language modeling loss and SquareHead loss for pretraining and PRG, the red line separates reconstruction stage from the continued training stage. **(Right)** Wikitext validation perplexity for training GPT2 under different settings.

#### 4.1 Two Stages of PRG

Unlike pretraining language models from scratch, the process of retraining a sparse model can be divided into two distinct stages based on the characteristics of the training process: the **Reconstruction Stage** and the **Continue Training Stage**. The sparse model is initialized with dense pretrained weight, and the sparsity mask  $m(W)$  calculated based on magnitude.

During the reconstruction stage, the model quickly relearns lost knowledge due to initial pruning. As a result, both training and validation losses decrease much faster compared with pretraining from scratch. Additionally, despite back-propagating with only language modeling loss, the SquareHead loss which measures the difference in intermediate outputs also decreases at the start of training. As shown in Fig. 2, these two phenomena occur during the same period in training. Therefore, we believe this stage should be distinguished from the later continue training stage, which more closely resembles traditional pretraining where the loss decreases slowly and SquareHead loss increases as the model learns new features.

A plausible explanation for this is that, unlike randomly initialized models, **the pruned model retains a portion of the knowledge acquired during pretraining. However, its expressive capacity is diminished due to the pruning process**. Therefore, in the reconstruction stage of PRG, the model focuses on recovering its expressive ability, allowing it to demonstrate its hidden knowledge. "Since the expressive ability is somewhat universal, the SquareHead loss, which measures the difference between hidden states, decreases at the start. Moreover, as recovering knowledge is faster than learning it from scratch, this accounts for the rapid decrease in loss. After the model recovers its expressive ability, it will move on to the continue training stage where it slowly learns new knowledge, resulting in an increase in SquareHead loss and the deceleration of the loss drop.

#### 4.2 Knowledge Distillation

During PRG training, relying solely on language modeling loss is insufficient for a pruned model to converge to an optimal state, especially for smaller language models like GPT-2 or OPT-125M. As shown in Figure 2, the loss curve is unstable, and perplexity remains high without distillation. This instability occurs because, during the reconstruction stage, pruned models are more susceptible to overfitting on the limited amount of data available at the start, which prevents them from learning global features and converging to an optimal state later on. It should be noted that unlike traditional overfitting, this phenomenon persists even when a much smaller learning rate than that used in pretraining is selected, and therefore it cannot be resolved by simply reducing the learning rate.

To address this issue, we found that applying KL-divergence loss is adequate to prevent the model from achieving sub-optimal results. Unlike language modeling loss, KL-divergence loss quantifies the

difference between two probability distributions and provides richer signals, thus helping to prevent the model from overfitting at the beginning. On the other hand, we find that applying SquareHead loss to intermediate outputs can limit the sparse model from achieving better results, contrary to findings in Sparse Fine-tuning [28]. We believe that while adding restraints to intermediate outputs may be beneficial when fine-tuning sparse models for downstream tasks, it can hinder the model’s generalization ability. Therefore, we apply the following loss function:

$$\mathcal{L} = \mathcal{L}_{task} + \alpha \mathcal{L}_{logit} = - \sum_{i=1}^{B*S} \log p_{\theta_s}(x_i) + \alpha D_{KL}(\theta_t || \theta_s)$$

As overfitting is more severe in smaller models, we typically apply a larger  $\alpha$  for these models.

### 4.3 Annealing SR-STE

A naive method for retraining sparse models, as used in Wanda [45], involves freezing the mask at the beginning of training and only updating the unmasked weights. However, choosing a permanent mask based on one-shot pruning prevents a smooth transition from a dense to a sparse model and, more importantly, discards all knowledge stored in the pruned weights, thereby inhibiting convergence speed and leading to sub-optimal results. As a solution, we allow the model to dynamically determine the mask during training. Existing work [21, 33, 53] on dynamic mask training has already proven that the flip ratio of a healthy PRG training process should be higher at the beginning and then gradually decrease. Additionally, they employ SR-STE [53] as a powerful method for adjusting the flip ratio to achieve optimal results.

Nonetheless, we argue that the current constant SR-STE decay factor does not fully tap into the potential of sparse models. Inspired by the Simulated Annealing (SA) algorithm [3], we believe that the decay factor plays a role similar to temperature in the SA algorithm. When the decay factor is relatively high, the weights that are masked receive a greater decay signal, thereby reducing their likelihood of being selected in subsequent mask choices. This leads to a decrease in the flip ratio, and vice versa. At the beginning of training, it is beneficial for the model to explore a variety of mask choices more extensively, which necessitates a lower decay factor. In the later stages of training, to facilitate better convergence, we prefer less variation in the mask, requiring a higher decay factor. Therefore, we propose a novel dynamic decay factor scheduler named **Annealing SR-STE**.

The decay factor for batch  $t$  is:

$$\lambda_W(t) = \begin{cases} \alpha t, & \text{if } 0 \leq t \leq T_0 \\ \alpha T_0, & \text{if } T_0 \leq t \leq T_1 \end{cases}$$

Here,  $T_0$  denotes the total number of training batches, and  $T_1$  represents the increasing decay batch. Although the loss may decrease more slowly at the beginning due to frequent mask changes, applying Annealing SR-STE can eventually surpass the original method and reduce up to 30% of the performance gap in the GPT-2 model compared with static SR-STE. Details of the flip rate and initial flip rate during training are provided in Figure 4.

### 4.4 Sparse Low-Rank Boosting

The pruned model with 2:4 sparsity, which retains only half of the parameters under a strict structural constraint, experiences a reduction in expressive capacity. To mitigate this issue, we incorporate a LoRA (Low-Rank Adaptation) [20] shape parameter that trains in conjunction with the original parameters, helping to bridge the performance gap between dense and sparse models with minimal memory increase. Unlike typical LoRA fine-tuning approaches where the original model parameters are frozen and only the adapters are trained, our strategy involves training both the sparse parameters and the adapter weights simultaneously. This deviation is due to the fact that in classic LoRA fine-tuning, the extra weights are trained for downstream tasks, and the original model is frozen to prevent over-fitting and catastrophic forgetting. However, in our approach, both the additional weights and the original model are trained on a pretraining dataset to enhance generalization capabilities, allowing for their concurrent training.

Specifically, for a weight matrix of size  $N \times d$  we choose the rank  $r$  to be  $\frac{d}{k}$  where  $k$  can be 64, 32, 16 and so on. A smaller  $k$  will yield better performance but will also require more memory. We named

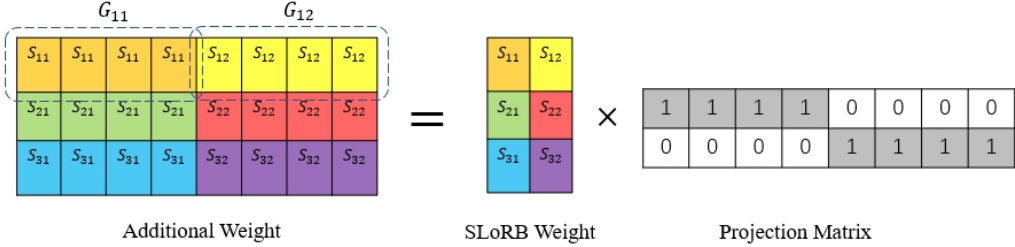


Figure 3: Visualization of SLoRB Initialization. Suppose the weight matrix is a 3 by 8 matrix and  $k = 4$ . We choose  $S_{ij}$  to be the mean of all the pruned weights in the Group  $G_{ij}$ . Therefore, the equivalent weight matrix with SLoRB weights can retain the same mean as the original matrix for each group.

this method **Sparse Low-Rank Boosting (SLoRB)**, which trades memory overhead for performance.

Another feature for our method is the initialization methods. Classic LoRA typically employs random initialization methods such as Xavier initialization [11] or Kaiming initialization [18]. However, in our case, we utilize the pruned weights as additional information to initialize SLoRB weights, thereby accelerating training. Given that in 2:4 sparsity, each neuron can only access half of the inputs, we find that adding additional information that reflects the weight's global features can help preserve model capacity. Specifically for a weight matrix  $W$  with size of  $N \times d$  and its mask matrix  $M$ , we select projection matrix  $X$  of size  $\frac{d}{k} \times d$  and a SLoRB weight matrix  $S$  of size  $N \times \frac{d}{k}$ .  $X$  and  $S$  are defined as follows::

$$x_{ij} = \begin{cases} 1, & \text{if } i \cdot k \leq j \leq (i+1) \cdot k - 1 \\ 0, & \text{otherwise} \end{cases}$$

As shown in Fig 3, each SLoRB weight is broadcast within Group  $G_{ij}$ . By setting  $S_{ij}$  as the mean of all pruned weights in group  $G_{ij}$ , this design ensures the mean values in groups  $G_{ij}$  remain consistent after pruning. We find that this initialization method enables the model to have a better start in training, as shown in Table 7. Although different initialization methods ultimately converge to similar results given sufficient training steps, our SLoRB initialization converges faster and is particularly useful when the computational budget is limited.

## 5 Compressing Models with Different Semi-structured Sparsity Pattern

In this section, we discuss the potential to compress models using semi-structured sparsity patterns. Previously, we examined 2:4 patterns, but theoretically, any N:M pattern can enhance matrix multiplication with appropriate hardware support. With that said, patterns with looser constraints (i.e., a larger M) often perform better but are more challenging to compress effectively. We aim to identify the optimal trade-off and, to maintain fairness in comparison, we focus only on patterns that achieve a 50% sparsity ratio, such as 2:4, 4:8, etc.

It should be noted that deploying semi-structured sparse models can lead to potential memory overhead. Take the 2:4 sparsity pattern as an example: although only two non-zero elements out of every four weights need to be stored, additional positional information is required to correctly restore these compressed weights to the original matrix for calculations. Storing these indices will consume an additional proportion of memory. A naive method would be to store one bit as a mask for each element, which results in a 50% memory overhead with a 4-bit quantized model at 50% sparsity. However, a more efficient approach exists: since there are 2 non-zero elements, there are a total of  $\binom{4}{2} = 6$  possible positions, hence only an additional 3 bits are sufficient.

We define the compression ratio as the percentage of memory latency of the compressed model compared to the original model. In our setting we compress dense models with FP32 precision to 4-bit model with  $n:2n$  semi-structured sparsity, therefore the compression ratio can be formulated as:

$$C_n = \frac{n * 4 + \lceil \log_2 \binom{2n}{n} \rceil (bit)}{2n * 32(bit)} = \frac{1}{16} + \frac{\lceil \log_2 \binom{2n}{n} \rceil}{64n}$$

Through mathematical formulation A.1 we can provide an approximate upper bound for compression ratio and as well as an predicted actual compression ratio when extending to sparsity patterns with larger  $N$  and  $M$ .

$$\log_2 \binom{2n}{n} = \log_2 \frac{(2n)!}{(n!)^2} \leq \log_2 \frac{4^n}{\sqrt{\pi n}} = 2n - \log_2 \sqrt{\pi n}$$

If we remove ceiling function for approximation

$$C_n \approx \frac{3}{32} - \frac{\log_2 \sqrt{\pi n}}{64n}$$

Therefore, the compression ratio is approximately an increasing function with an upper bound of  $C^* = \frac{3}{32} \approx 9.375\%$ . In practice, to further enhance compression, we can employ Huffman Encoding, similar to what was done in Deep Compression [14]. We construct a Huffman Tree with evenly distributed frequencies, as empirical results support our claim. The actual compression ratios are shown in Table 1. We observe that as  $n$  increases, performance improves; however, although the compression ratio increases, it remains below the upper bound.

Table 1: Comparison of perplexity and compression ratio of different sparsity pattern.

Sparsity Pattern	1:2	2:4	4:8	8:16	16:32	32:64	Unstructured 50%
Perplexity	32.56	31.13	30.73	30.37	30.34	30.32	30.18
Actual Compression Ratio	7.81%	8.33%	8.66%	8.93%	9.10%	9.22%	-

## 6 Results

### 6.1 Experiment Setup

**Model configurations.** We tested our methods on three different LLM model families: LLAMA2-7B [46], OPT 125M/350M/1.3B [50], and GPT2 models[4]. The LLAMA2-7B model was trained on eight Nvidia H800 GPUs with 80 GB of memory, while the OPT and GPT2 models were trained on L20 GPUs with 48 GB of memory. The training script for the GPT2 and OPT models was modified from the nanoGPT library [24], whereas the training script for LLAMA2-7B was modified from ShearedLLAMA [48]. We present our experimental results for two different sparsity patterns: AST-Naive, which is trained without additional weight and adheres to a strict 2:4 sparsity pattern, and AST-Boosted, which is trained with extra SLoRB weight to trade memory for precision. We select  $k = 16$  which adds a total of 12.5% of extra parameter. We locate best hyper-parameters through grid search. The best hyper-parameters and training details are presented in Appendix A.2.

**Data.** For training smaller models in the OPT and GPT2 families, we used the C4 dataset [40]. For the LLAMA2-7B models, we employed a more comprehensive dataset named RedPajama-v1<sup>1</sup>, which comprises data from seven domains: CommonCrawl, C4, Github, Wikipedia, Books, ArXiv, and StackExchange. Additionally, we utilized the dynamic batching feature provided in the ShearedLLAMA codebase. We adhered to the train-eval split presented in ShearedLLAMA.

**Baseline.** We compare our methods with other models featuring N:M sparsity, including SparseGPT[9] and Wanda [45]. Both Wanda and SparseGPT require calibration data. To ensure fairness, we use the calibration data provided in their codebase.

<sup>1</sup><https://huggingface.co/datasets/togethercomputer/RedPajama-Data-1T>

**Evaluation.** We tested the WikiText-2 perplexity for all models and assessed zero-shot and few-shot performance using EleutherAI’s LM Harness [10] on LLAMA2-7B. Our evaluation tasks include: zero-shot ARC Easy [6], OpenBookQA [34], WinoGrande [42], RTE from the GLUE benchmark [47], HellaSwag [49], ARC Challenge [6], BoolQ [5], and five-shot performance on the Massive Multitask Language Understanding (MMLU) [19].

## 6.2 Language Modeling

In Table 2, we compared the perplexity results of our sparse models with the Wanda and SparseGPT baselines. We employed the same procedure as described in their original papers to obtain any results that were not provided.

Our method, AST-Naive, which maintains the same sparsity pattern as the baseline, can significantly outperform previous methods by a large margin across various models. For instance, on smaller models like OPT-125M, where previous methods completely fail, AST-Naive can reduce the perplexity margin to 2.48, and AST-Boosted can further achieve an almost negligible margin of 0.92. For larger models, AST can still significantly reduce the gap; for the LLAMA2-7B model, our AST-Boost method achieved a perplexity increase of only 0.59. **It should be noted that our sparse models consistently outperform smaller dense models with a similar parameter count, suggesting a promising approach for obtaining parameter-efficient models.**

Table 2: Perplexity results on raw-WikiText2 on 2:4 Sparsified Language Model.

Method	Weight Update	LLAMA2		OPT			GPT2		
		7B	125M	350M	1.3B	124M	350M	774M	1.5B
Dense	-	5.12	27.76	22.00	14.62	29.95	21.72	19.43	17.40
SparseGPT	✓	10.17	45.58	40.33	29.03	50.09	31.03	25.98	21.14
Wanda	✗	11.02	60.91	50.16	23.92	115.64	63.71	49.97	30.44
AST-Naive(Ours)	✓	5.82	30.22	24.65	15.85	32.34	23.65	21.29	18.33
AST-Boosted(Ours)	✓	<b>5.69</b>	<b>28.68</b>	<b>24.03</b>	<b>15.43</b>	<b>31.13</b>	<b>23.03</b>	<b>20.66</b>	<b>18.01</b>

In addition, we provide the results for quantized sparse model in Appendix A.3.

## 6.3 Zero-shot and Few-shot Result

In Table 3, we present the results of zero-shot and few-shot accuracy. We have chosen the results reported in Wanda [45] as our baseline, where the models were trained either through LoRA fine-tuning or full parameter retraining, with masks frozen. Although not specifically reported, their computational cost is presumed to be similar to ours; Wanda trained for three days on 4 GPUs, while we trained for approximately two days on 8 GPUs. Our method performed best in most of the tasks. The primary reason for tasks where our models were outperformed is mainly attributed to the differences in the dense models used for training—Wanda used LLAMA, while we used LLAMA2—rather than differences in training methods.

In Table 4 we present the results for five-shot MMLU, as Wanda did not report results with training, we used results from one-shot pruning methods to be our baseline. Results show that one-shot pruning significantly loss zero-shot ability while our methods can manage to recover most of the lost generalization ability.

## 7 Conclusion

In this paper, we present a novel training pipeline for semi-structured sparse models named *Adaptive Sparse Trainer(AST)*. By distilling knowledge from the pruned model weights, AST mitigates overfitting and ensures a stable training process. Moreover, it enhances the identification of optimal lottery tickets (e.g., masks) by allowing the model to adaptively train masks. Additionally, we demonstrate that incorporating extra well-initialized parameters can further improve model performance with only a minimal increase in the memory footprint. Our work significantly narrows the precision gap in

Table 3: Accuracy (%) of LLAMA-7B and LLAMA2-7B on seven zero-shot tasks.

Models	Method	BoolQ	RTE	HellaSwag	WinoGrande	ARC-e	ARC-c	OBQA	Mean
LLAMA-7B	Dense	75.05	66.43	56.92	69.93	75.34	41.89	34.40	59.99
	Wanda (LoRA)	70.32	64.98	52.53	65.04	67.00	33.53	27.80	54.46
	Wanda (Full Param)	73.21	61.34	54.86	66.18	70.24	35.68	<b>31.80</b>	56.19
LLAMA2-7B	Dense	77.73	63.89	57.18	69.04	76.17	42.91	31.60	59.78
	AST-Naive	73.12	<b>66.06</b>	54.66	67.87	73.61	39.93	28.60	57.68
	AST-Boosted	<b>75.04</b>	<b>66.06</b>	<b>55.24</b>	<b>68.48</b>	<b>74.91</b>	<b>41.11</b>	29.40	<b>58.62</b>

Table 4: Accuracy (%) of MMLU for LLAMA2-7B models with 2:4 sparsity.

LLAMA2-7B	Dense	SparseGPT	Wanda	AST-Naive	AST-Boosted
<b>MMLU(5-shot)</b>	45.3	27.5	27.6	37.9	38.2

terms of both perplexity and zero-shot accuracy between dense and semi-structured sparse models with minimal training cost. We also conducted a theoretical analysis for compressing models with N:M sparsity.

We hope our work contributes to a better understanding of retraining pruned models. However, due to computational constraints, we employed a minimal number of training tokens. It would be interesting to further investigate AST’s performance with larger models or by training with more tokens.

## References

- [1] Josh Achiam, Steven Adler, Sandhini Agarwal, Lama Ahmad, Ilge Akkaya, Florencia Leoni Aleman, Diogo Almeida, Janko Altenschmidt, Sam Altman, Shyamal Anadkat, et al. Gpt-4 technical report. *arXiv preprint arXiv:2303.08774*, 2023.
- [2] Yoshua Bengio, Nicholas Léonard, and Aaron Courville. Estimating or propagating gradients through stochastic neurons for conditional computation. *arXiv preprint arXiv:1308.3432*, 2013.
- [3] Dimitris Bertsimas and John Tsitsiklis. Simulated annealing. *Statistical science*, 8(1):10–15, 1993.
- [4] Tom Brown, Benjamin Mann, Nick Ryder, Melanie Subbiah, Jared D Kaplan, Prafulla Dhariwal, Arvind Neelakantan, Pranav Shyam, Girish Sastry, Amanda Askell, et al. Language models are few-shot learners. *Advances in neural information processing systems*, 33:1877–1901, 2020.
- [5] Christopher Clark, Kenton Lee, Ming-Wei Chang, Tom Kwiatkowski, Michael Collins, and Kristina Toutanova. Boolq: Exploring the surprising difficulty of natural yes/no questions. *CoRR*, abs/1905.10044, 2019.
- [6] Peter Clark, Isaac Cowhey, Oren Etzioni, Tushar Khot, Ashish Sabharwal, Carissa Schoenick, and Oyvind Tafjord. Think you have solved question answering? try arc, the ai2 reasoning challenge. *arXiv preprint arXiv:1803.05457*, 2018.
- [7] Jacob Devlin, Ming-Wei Chang, Kenton Lee, and Kristina Toutanova. Bert: Pre-training of deep bidirectional transformers for language understanding. *arXiv preprint arXiv:1810.04805*, 2018.
- [8] Elias Frantar and Dan Alistarh. Spdy: Accurate pruning with speedup guarantees. In *International Conference on Machine Learning*, pages 6726–6743. PMLR, 2022.
- [9] Elias Frantar and Dan Alistarh. Sparsegpt: Massive language models can be accurately pruned in one-shot. In *International Conference on Machine Learning*, pages 10323–10337. PMLR, 2023.

[10] Leo Gao, Jonathan Tow, Stella Biderman, Sid Black, Anthony DiPofi, Charles Foster, Laurence Golding, Jeffrey Hsu, Kyle McDonell, Niklas Muennighoff, et al. A framework for few-shot language model evaluation. *Version v0. 0.1. Sept*, page 8, 2021.

[11] Xavier Glorot and Yoshua Bengio. Understanding the difficulty of training deep feedforward neural networks. In *Proceedings of the thirteenth international conference on artificial intelligence and statistics*, pages 249–256. JMLR Workshop and Conference Proceedings, 2010.

[12] Jianping Gou, Baosheng Yu, Stephen J Maybank, and Dacheng Tao. Knowledge distillation: A survey. *International Journal of Computer Vision*, 129(6):1789–1819, 2021.

[13] Jinyang Guo, Jianyu Wu, Zining Wang, Jiaheng Liu, Ge Yang, Yifu Ding, Ruihao Gong, Haotong Qin, and Xianglong Liu. Compressing large language models by joint sparsification and quantization. In *Forty-first International Conference on Machine Learning*, 2024.

[14] Song Han, Huizi Mao, and William J Dally. Deep compression: Compressing deep neural networks with pruning, trained quantization and huffman coding. *arXiv preprint arXiv:1510.00149*, 2015.

[15] Song Han, Jeff Pool, John Tran, and William Dally. Learning both weights and connections for efficient neural network. In C. Cortes, N. Lawrence, D. Lee, M. Sugiyama, and R. Garnett, editors, *Advances in Neural Information Processing Systems*, volume 28. Curran Associates, Inc., 2015.

[16] Song Han, Jeff Pool, John Tran, and William Dally. Learning both weights and connections for efficient neural network. *Advances in neural information processing systems*, 28, 2015.

[17] Babak Hassibi, David G Stork, and Gregory J Wolff. Optimal brain surgeon and general network pruning. In *IEEE international conference on neural networks*, pages 293–299. IEEE, 1993.

[18] Kaiming He, Xiangyu Zhang, Shaoqing Ren, and Jian Sun. Delving deep into rectifiers: Surpassing human-level performance on imagenet classification. In *Proceedings of the IEEE international conference on computer vision*, pages 1026–1034, 2015.

[19] Dan Hendrycks, Collin Burns, Steven Basart, Andy Zou, Mantas Mazeika, Dawn Song, and Jacob Steinhardt. Measuring massive multitask language understanding. *arXiv preprint arXiv:2009.03300*, 2020.

[20] Edward J. Hu, Yelong Shen, Phillip Wallis, Zeyuan Allen-Zhu, Yuanzhi Li, Shean Wang, Lu Wang, and Weizhu Chen. Lora: Low-rank adaptation of large language models, 2021.

[21] Yuezhou Hu, Kang Zhao, Weiyu Huang, Jianfei Chen, and Jun Zhu. Accelerating transformer pre-training with 2:4 sparsity, 2024.

[22] Itay Hubara, Brian Chmiel, Moshe Island, Ron Banner, Joseph Naor, and Daniel Soudry. Accelerated sparse neural training: A provable and efficient method to find  $n: m$  transposable masks. *Advances in neural information processing systems*, 34:21099–21111, 2021.

[23] Ajay Jaiswal, Zhe Gan, Xianzhi Du, Bowen Zhang, Zhangyang Wang, and Yinfei Yang. Compressing llms: The truth is rarely pure and never simple, 2024.

[24] Andrej Karpathy. nanogpt. <https://github.com/karpathy/nanoGPT/>, 2023.

[25] Diederik P Kingma and Jimmy Ba. Adam: A method for stochastic optimization. *arXiv preprint arXiv:1412.6980*, 2014.

[26] Solomon Kullback and Richard A Leibler. On information and sufficiency. *The annals of mathematical statistics*, 22(1):79–86, 1951.

[27] Eldar Kurtic and Dan Alistarh. Gmp\*: Well-tuned gradual magnitude pruning can outperform most bert-pruning methods. *arXiv preprint arXiv:2210.06384*, 2022.

[28] Eldar Kurtic, Denis Kuznedelev, Elias Frantar, Michael Goin, and Dan Alistarh. Sparse finetuning for inference acceleration of large language models. *arXiv preprint arXiv:2310.06927*, 2023.

[29] Yann LeCun, John Denker, and Sara Solla. Optimal brain damage. *Advances in neural information processing systems*, 2, 1989.

[30] Ji Lin, Jiaming Tang, Haotian Tang, Shang Yang, Xingyu Dang, and Song Han. Awq: Activation-aware weight quantization for llm compression and acceleration. *arXiv preprint arXiv:2306.00978*, 2023.

[31] Zhuang Liu, Jianguo Li, Zhiqiang Shen, Gao Huang, Shoumeng Yan, and Changshui Zhang. Learning efficient convolutional networks through network slimming. In *Proceedings of the IEEE international conference on computer vision*, pages 2736–2744, 2017.

[32] Zhuang Liu, Mingjie Sun, Tinghui Zhou, Gao Huang, and Trevor Darrell. Rethinking the value of network pruning. *arXiv preprint arXiv:1810.05270*, 2018.

[33] Yucheng Lu, Shivani Agrawal, Suvinay Subramanian, Oleg Rybakov, Christopher De Sa, and Amir Yazdanbakhsh. Step: Learning n: M structured sparsity masks from scratch with precondition. In *International Conference on Machine Learning*, pages 22812–22824. PMLR, 2023.

[34] Todor Mihaylov, Peter Clark, Tushar Khot, and Ashish Sabharwal. Can a suit of armor conduct electricity? a new dataset for open book question answering. *arXiv preprint arXiv:1809.02789*, 2018.

[35] Pavlo Molchanov, Arun Mallya, Stephen Tyree, Iuri Frosio, and Jan Kautz. Importance estimation for neural network pruning. In *Proceedings of the IEEE/CVF conference on computer vision and pattern recognition*, pages 11264–11272, 2019.

[36] Azade Nova, Hanjun Dai, and Dale Schuurmans. Gradient-free structured pruning with unlabeled data. In *International Conference on Machine Learning*, pages 26326–26341. PMLR, 2023.

[37] Aleksandra I. Nowak, Bram Grooten, Decebal Constantin Mocanu, and Jacek Tabor. Fantastic weights and how to find them: Where to prune in dynamic sparse training, 2023.

[38] Mansheej Paul, Feng Chen, Brett W Larsen, Jonathan Frankle, Surya Ganguli, and Gintare Karolina Dziugaite. Unmasking the lottery ticket hypothesis: What’s encoded in a winning ticket’s mask? *arXiv preprint arXiv:2210.03044*, 2022.

[39] Mary Phuong and Christoph Lampert. Towards understanding knowledge distillation. In *International conference on machine learning*, pages 5142–5151. PMLR, 2019.

[40] Colin Raffel, Noam Shazeer, Adam Roberts, Katherine Lee, Sharan Narang, Michael Matena, Yanqi Zhou, Wei Li, and Peter J Liu. Exploring the limits of transfer learning with a unified text-to-text transformer. *Journal of machine learning research*, 21(140):1–67, 2020.

[41] Alex Renda, Jonathan Frankle, and Michael Carbin. Comparing rewinding and fine-tuning in neural network pruning. *arXiv preprint arXiv:2003.02389*, 2020.

[42] Keisuke Sakaguchi, Ronan Le Bras, Chandra Bhagavatula, and Yejin Choi. Winogrande: An adversarial winograd schema challenge at scale. *Communications of the ACM*, 64(9):99–106, 2021.

[43] Maying Shen, Hongxu Yin, Pavlo Molchanov, Lei Mao, Jianna Liu, and Jose M Alvarez. Structural pruning via latency-saliency knapsack. *Advances in Neural Information Processing Systems*, 35:12894–12908, 2022.

[44] Sidak Pal Singh and Dan Alistarh. Woodfisher: Efficient second-order approximation for neural network compression. In H. Larochelle, M. Ranzato, R. Hadsell, M.F. Balcan, and H. Lin, editors, *Advances in Neural Information Processing Systems*, volume 33, pages 18098–18109. Curran Associates, Inc., 2020.

[45] Mingjie Sun, Zhuang Liu, Anna Bair, and J Zico Kolter. A simple and effective pruning approach for large language models. *arXiv preprint arXiv:2306.11695*, 2023.

[46] Hugo Touvron, Louis Martin, Kevin Stone, Peter Albert, Amjad Almahairi, Yasmine Babaei, Nikolay Bashlykov, Soumya Batra, Prajjwal Bhargava, Shruti Bhosale, Dan Bikel, Lukas Blecher, Cristian Canton Ferrer, Moya Chen, Guillem Cucurull, David Esiobu, Jude Fernandes, Jeremy Fu, Wenyin Fu, Brian Fuller, Cynthia Gao, Vedanuj Goswami, Naman Goyal, Anthony Hartshorn, Saghar Hosseini, Rui Hou, Hakan Inan, Marcin Kardas, Viktor Kerkez, Madiam Khabsa, Isabel Kloumann, Artem Korenev, Punit Singh Koura, Marie-Anne Lachaux, Thibaut Lavril, Jenya Lee, Diana Liskovich, Yinghai Lu, Yuning Mao, Xavier Martinet, Todor Mihaylov, Pushkar Mishra, Igor Molybog, Yixin Nie, Andrew Poulton, Jeremy Reizenstein, Rashi Rungta, Kalyan Saladi, Alan Schelten, Ruan Silva, Eric Michael Smith, Ranjan Subramanian, Xiaqing Ellen Tan, Binh Tang, Ross Taylor, Adina Williams, Jian Xiang Kuan, Puxin Xu, Zheng Yan, Iliyan Zarov, Yuchen Zhang, Angela Fan, Melanie Kambadur, Sharan Narang, Aurelien Rodriguez, Robert Stojnic, Sergey Edunov, and Thomas Scialom. Llama 2: Open foundation and fine-tuned chat models, 2023.

[47] Alex Wang, Amanpreet Singh, Julian Michael, Felix Hill, Omer Levy, and Samuel R Bowman. Glue: A multi-task benchmark and analysis platform for natural language understanding. *arXiv preprint arXiv:1804.07461*, 2018.

[48] Mengzhou Xia, Tianyu Gao, Zhiyuan Zeng, and Danqi Chen. Sheared llama: Accelerating language model pre-training via structured pruning. *arXiv preprint arXiv:2310.06694*, 2023.

[49] Rowan Zellers, Ari Holtzman, Yonatan Bisk, Ali Farhadi, and Yejin Choi. Hellaswag: Can a machine really finish your sentence? *arXiv preprint arXiv:1905.07830*, 2019.

[50] Susan Zhang, Stephen Roller, Naman Goyal, Mikel Artetxe, Moya Chen, Shuhui Chen, Christopher Dewan, Mona Diab, Xian Li, Xi Victoria Lin, Todor Mihaylov, Myle Ott, Sam Shleifer, Kurt Shuster, Daniel Simig, Punit Singh Koura, Anjali Sridhar, Tianlu Wang, and Luke Zettlemoyer. Opt: Open pre-trained transformer language models, 2022.

[51] Yingtao Zhang, Haoli Bai, Haokun Lin, Jialin Zhao, Lu Hou, and Carlo Vittorio Cannistraci. Plug-and-play: An efficient post-training pruning method for large language models. In *The Twelfth International Conference on Learning Representations*, 2024.

[52] Yuxin Zhang, Lirui Zhao, Mingbao Lin, Yunyun Sun, Yiwu Yao, Xingjia Han, Jared Tanner, Shiwei Liu, and Rongrong Ji. Dynamic sparse no training: Training-free fine-tuning for sparse llms. *arXiv preprint arXiv:2310.08915*, 2023.

[53] Aojun Zhou, Yukun Ma, Junnan Zhu, Jianbo Liu, Zhijie Zhang, Kun Yuan, Wenxiu Sun, and Hongsheng Li. Learning n: m fine-grained structured sparse neural networks from scratch. *arXiv preprint arXiv:2102.04010*, 2021.

[54] Yefan Zhou, Yaoqing Yang, Arin Chang, and Michael W Mahoney. A three-regime model of network pruning. In *International Conference on Machine Learning*, pages 42790–42809. PMLR, 2023.

[55] Michael Zhu and Suyog Gupta. To prune, or not to prune: exploring the efficacy of pruning for model compression, 2017.

## A Appendix

### A.1 Proof for Upper Bound of Combination Number

Proofs are sourced from Stack Exchange<sup>2</sup>. We have the follow equation:

$$\frac{1}{4^n} \binom{2n}{n} = \frac{(2n-1)!!}{(2n)!!} = \prod_{k=1}^n \left(1 - \frac{1}{2k}\right)$$

We square both sides of the equation:

---

<sup>2</sup><https://math.stackexchange.com/questions/1442351/stirling-approximation-of-binom2nn>

$$\left(\frac{1}{4^n} \binom{2n}{n}\right)^2 = \frac{1}{4} \prod_{k=2}^n \left(1 - \frac{1}{2k}\right)^2 = \frac{1}{4n} \prod_{k=1}^{n-1} \left(1 - \frac{1}{(2k+1)^2}\right)^{-1}$$

Using the Weierstrass product for the cosine function, we obtain:

$$\prod_{k=1}^{\infty} \left(1 - \frac{1}{(2k+1)^2}\right)^{-1} = \frac{4}{\pi}$$

Hence, it follows that:

$$\left(\frac{1}{4^n} \binom{2n}{n}\right)^2 = \frac{1}{\pi n} \prod_{k \geq n}^n \left(1 - \frac{1}{(2k+1)^2}\right)^{-1} = \frac{1}{\pi n} \prod_{k \geq n}^n \left(1 + \frac{1}{(2k+2)2k}\right)^{-1}$$

Therefore we have

$$\frac{1}{\sqrt{\pi n}} \geq \frac{1}{4^n} \binom{2n}{n}$$

## A.2 Hyperparamters

In this section, we present the hyper-parameters and the number of tokens used to train our model in Table 5.

Table 5: Hyperparameters and number of tokens used for training.

	OPT			GPT2				LLAMA2
Learning Rate	125M	350M	1.3B	124M	350M	774M	1.5B	7B
SR-STE	1e-4	1e-4	2e-5	2e-4	1e-4	1e-4	6e-5	2e-5
Training Steps	3e-4	1e-4	6e-5	1e-4	6e-5	6e-5	6e-5	6e-5
Total Flipped Ratio	40k	40k	20k	40k	40k	40k	20k	15k
KI loss parameter	11.1%	9.3%	4.4%	6.7%	3.6%	3.4%	4.2%	3.8%
Tokens Trained	2.0	2.0	2.0	2.0	2.0	2.0	2.0	0.5
	10B	10B	5B	5B	5B	5B	2.5B	7.5B

## A.3 Model Compression Using AWQ

In this section, we provide the perplexity results for quantized models using AWQ. The results in Table 6 show that our model can maintain performance even when extremely compressed. According to the results, the jointly compressed models using AWQ and AST can achieve state-of-the-art performance in extremely compressed domains.

## A.4 SLoRB Initialization

We conducted an ablation study on different initialization methods, training all models on GPT2 using SLoRB with specified computation limits of 1B, 2.5B, and 5B tokens—each ensuring respective convergence. The results are provided in Table 7. ‘Mean’ refers to the method discussed in the paper, while ‘Zero’ denotes initialization of both matrices from zero.

## A.5 Flip Rate During Training

In this section, we compare the flip rates and initial flip rates of static SR-STE and Annealing SR-STE. In our experiments, we update the mask and calculate the flip rate and initial flip rate

Table 6: Wikitext-2 perplexity for quantized sparse models.

Method	Theoretical Memory OverHead	LLAMA2		OPT		GPT2		
		7B	125M	1.3B	124M	350M	774M	1.5B
Dense	1.0x	5.12	27.76	14.62	29.95	21.72	19.43	17.40
AWQ-4bit	0.125x	5.68	29.12	14.95	31.93	22.66	19.89	17.80
AWQ-2bit	0.0675x	2.2e5	216.11	53.42	751.15	453.45	70.36	46.17
AST-Naive-8bit	0.125x	6.37	30.26	15.86	32.36	23.66	21.29	18.34
AST-Naive-4bit	0.0675x	6.48	31.28	16.05	34.00	24.39	21.72	18.60
AST-Boosted-4bit	0.078x	6.25	29.88	15.63	32.76	23.87	21.40	18.31

Table 7: Results of perplexity using different initialization methods with fixed training tokens.

Trained Token	0	1B	2.5B	5B
Mean	475.05	32.78	31.78	31.13
Xavier Uniform	720.74	33.22	31.82	31.15
Zero	720.74	33.43	32.93	32.46

every 10 batches during training, as more frequent recalculations do not enhance accuracy and increase computational overhead. Figure 4 4 illustrates the flip rates and initial flip rates during the retraining of the GPT2 model. Unlike traditional static decay factors, Annealing SR-STE modifies a higher percentage of its mask at the beginning, allowing the model to explore various mask patterns. Furthermore, Annealing SR-STE enables a more stable mask towards the end of training, fostering better convergence. Consequently, Annealing SR-STE supports a higher rate of mask changes (e.g., initial flip rate) while maintaining overall stability.

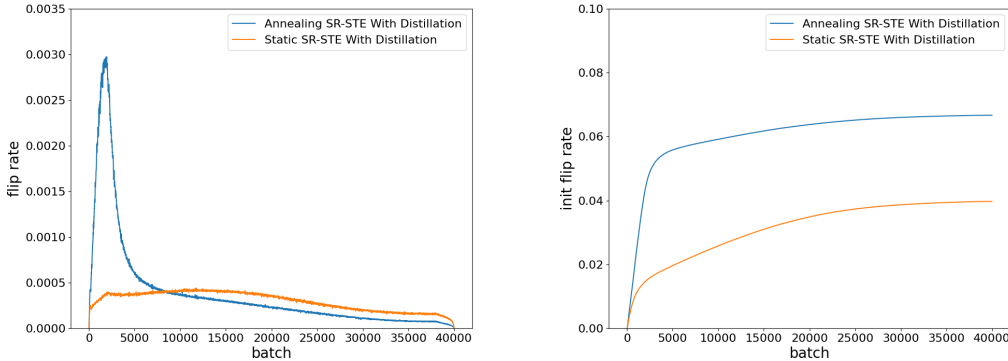


Figure 4: (Left) Flip rate for static and Annealing SR-STE during the training of the GPT2 model. (Right) Initial flip rate for static and Annealing SR-STE during the training of the GPT2 model.

## A.6 Broader Impact

AST can convert a densely pre-trained model into a 2:4 sparse model using weaker datasets without significant loss of model capacity. This 2:4 sparse model can then be used for accelerated inference. This enables the deployment of large-scale models at a lower cost or with increased speed, and potentially allows larger models to run on less powerful hardware. However, this technique could also be used to train models that generate harmful content, such as content that violates AI ethics.